

Synthesis, crystal structure and Hirshfeld surface analysis of 2-phenyl-3-(prop-2-yn-1-yloxy)quinoxaline

Nadeem Abad,^{a,b} Joel T. Mague,^c Abdulsalam Alsubari,^{d*} El Mokhtar Essassi,^b Mehrdad Pourayoubi,^e Abdullah Yahya Abdullah Alzahrani^f and Youssef Ramli^{a,g*}

Received 6 March 2024

Accepted 19 March 2024

Edited by L. Van Meervelt, Katholieke Universiteit Leuven, Belgium

Keywords: crystal structure; quinoxaline; alkylation; hydrogen bond; π -stacking.

CCDC reference: 2142451

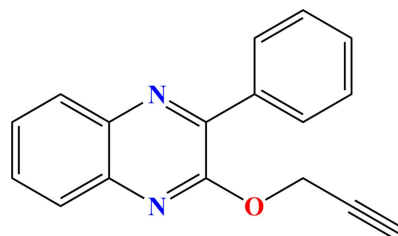
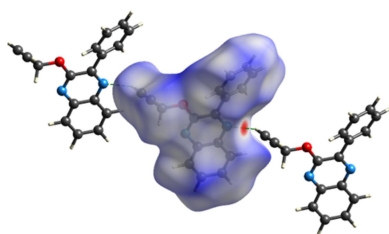
Supporting information: this article has supporting information at journals.iucr.org/e

^aLaboratory of Medicinal Chemistry, Drug Sciences Research Center, Faculty of Medicine and Pharmacy, Mohammed V University in Rabat, Morocco, ^bLaboratory of Heterocyclic Organic Chemistry, Faculty of Sciences, Mohammed V University, Rabat, Morocco, ^cDepartment of Chemistry, Tulane University, New Orleans, LA 70118, USA, ^dLaboratory of Medicinal Chemistry, Faculty of Clinical Pharmacy, 21 September University, Yemen, ^eDepartment of Chemistry, Faculty of Science, Ferdowsi University of Mashhad, Mashhad, Iran, ^fDepartment of Chemistry, Faculty of Science and Arts, King Khalid University, Mohail Assir, Saudi Arabia, and ^gMohammed VI Center for Research and Innovation (CM6), Rabat 10000, Morocco. *Correspondence e-mail: alsubaripharmaco@21umas.edu.ye, y.ramli@um5r.ac.ma

In the title compound, C₁₇H₁₂N₂O, the quinoxaline moiety shows deviations of 0.0288 (7) to −0.0370 (7) Å from the mean plane (r.m.s. deviation of fitted atoms = 0.0223 Å). In the crystal, corrugated layers two molecules thick are formed by C—H...N hydrogen bonds and π -stacking interactions.

1. Chemical context

Quinoxaline derivatives are described extensively among the heterocycles being investigated for the discovery and development of new biologically active molecules. Numerous studies have been published regarding this class of compounds, revealing that quinoxaline is present in a number of well-established drugs with diverse therapeutic activities as well as industrial properties (*e.g.* Lgaz *et al.*, 2015). In recent decades, the medicinal chemistry of quinoxaline and its derivatives have received great attention due to their wide spectrum of biological activities, in particular analgesic, anti-diabetic, antiviral, antibacterial, antioxidant, anti-inflammatory, antidepressant, and anti-tubercular (Ramli & Essassi, 2015). Our interest in quinoxalines results from their simple synthesis and the ease with which X-ray quality crystals can be grown. Following this line of research, and as a continuation of our work in this area (*e.g.* Missioui *et al.*, 2022), based on the therapeutic significance of this scaffold for potential applications in medicinal chemistry, we report herein the synthesis of a new quinoxaline derivative by an alkylation reaction of 3-phenylquinoxalin-2(1*H*)-one using 3-bromoprop-1-yne as an alkylating reagent and potassium carbonate in the presence of tetra-*n*-butylammonium bromide as catalyst in phase-transfer catalysis (Fig. 1). A Hirshfeld surface analysis was performed to analyze the intermolecular interactions.



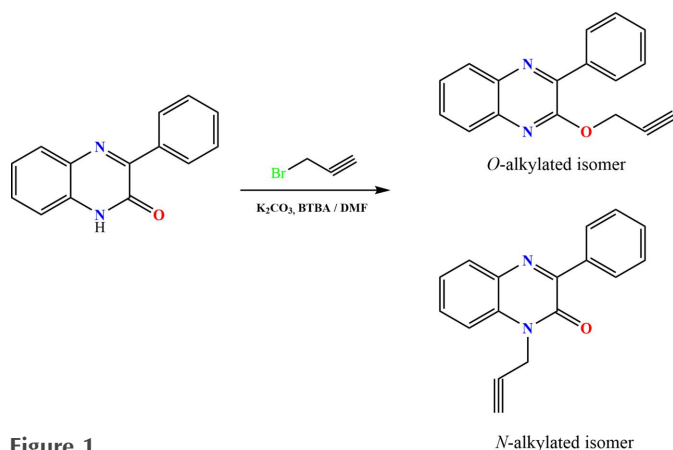


Figure 1
Synthesis of the title compound.

2. Structural commentary

In the title molecule, the fused bicyclic ring system is not entirely planar, as indicated by the dihedral angle of $2.25(6)^\circ$ between its constituent rings and by the deviations from the mean plane through the ten atoms, which range from $0.0288(7) \text{ \AA}$ (C8) to $-0.0370(7) \text{ \AA}$ (C2) (r.m.s. deviation of fitted atoms = 0.0223 \AA). The plane of the benzene ring C12–C17 is inclined to the above plane by $34.04(4)^\circ$, while the methylene carbon of the propynyl group (C9) lies virtually in the plane of the quinoxaline unit, as indicated by the C9–O1–C7–N1 torsion angle of $0.65(13)^\circ$. However, the propynyl group is almost perpendicular to the above plane, as indicated by the C7–O1–C9–C10 torsion angle of $-87.0(1)^\circ$ (Fig. 2).

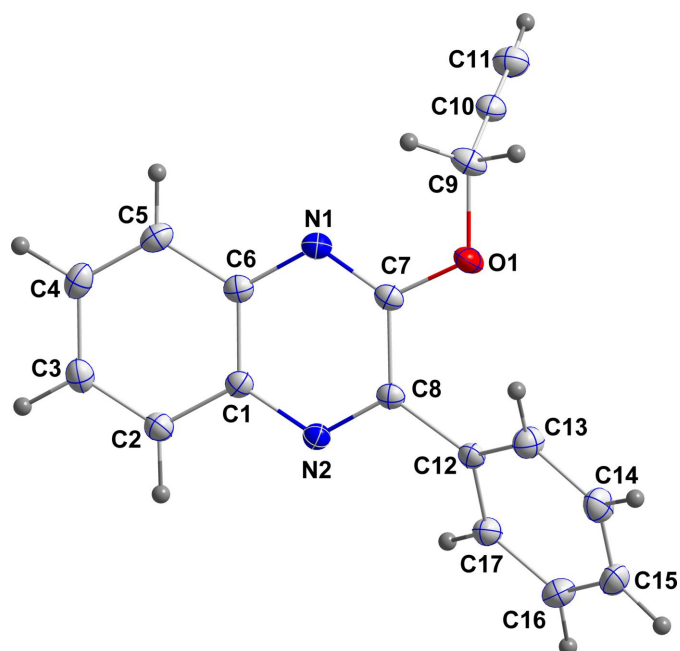


Figure 2
Molecular structure of the title molecule with labeling scheme and 50% probability ellipsoids.

Table 1
Hydrogen-bond geometry (\AA , $^\circ$).

$D-H \cdots A$	$D-H$	$H \cdots A$	$D \cdots A$	$D-H \cdots A$
C11–H11 \cdots N2 ⁱ	0.95	2.44	3.3164 (14)	153

Symmetry code: (i) $x, y + 1, z$.

3. Supramolecular features

In the crystal, the molecules are connected into chains extending along the b -axis direction by C11–H11 \cdots N2 hydrogen bonds (Table 1 and Fig. 3). The chains are linked into corrugated layers two molecules thick by offset π -stacking interactions between the C1–C6 and C1/C6/N1/C7/C8/N2 rings [centroid–centroid distance = $3.6716(8) \text{ \AA}$; dihedral angle = $2.25(4)^\circ$, slippage = 1.262 \AA] across inversion centers (Fig. 3).

To quantify the extent of each type of intermolecular interaction in the crystal packing, a Hirshfeld surface analysis was performed using *CrystalExplorer* (Version 21.5; Spackman *et al.*, 2021). Descriptions of the surfaces generated and their interpretation have been published (Tan *et al.*, 2019). Fig. 4 shows the d_{norm} surface with Fig. 4a showing two neighboring molecules illustrating the C–H \cdots N hydrogen bond and Fig. 4b one neighbor illustrating the π -stacking. From Fig. 4a, it is clear that the C–H \cdots N hydrogen bond is the only intermolecular hydrogen bond in the structure. Fig. 5a shows the surface mapped over shape-index while Fig. 5b shows it mapped over curvature. In both of these, the characteristic features of intermolecular π -stacking interactions are quite evident. Fig. 6 presents the 2D fingerprint plots with Fig. 6a giving the total of all intermolecular interactions and Fig. 6b–6e showing those delineated into H \cdots H, C \cdots H/H \cdots C, N \cdots H/H \cdots N and C \cdots C interactions. These are the major interactions and contribute 42.8%, 36.8%, 8.3% and 6.3% to the total, respectively. In the absence of C–H \cdots π (ring) interactions, the large contribution of C \cdots H/H \cdots C interactions may seem unusual, but *PLATON* (Spek, 2020) indicates that there are at least six and as many as ten

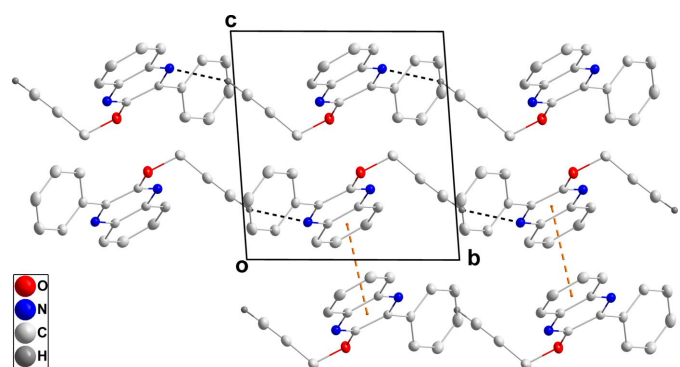


Figure 3
Packing viewed along the a -axis direction with C–H \cdots N hydrogen bonds and π -stacking interactions shown, respectively, by black and orange dashed lines. Non-interacting hydrogen atoms are omitted for clarity.

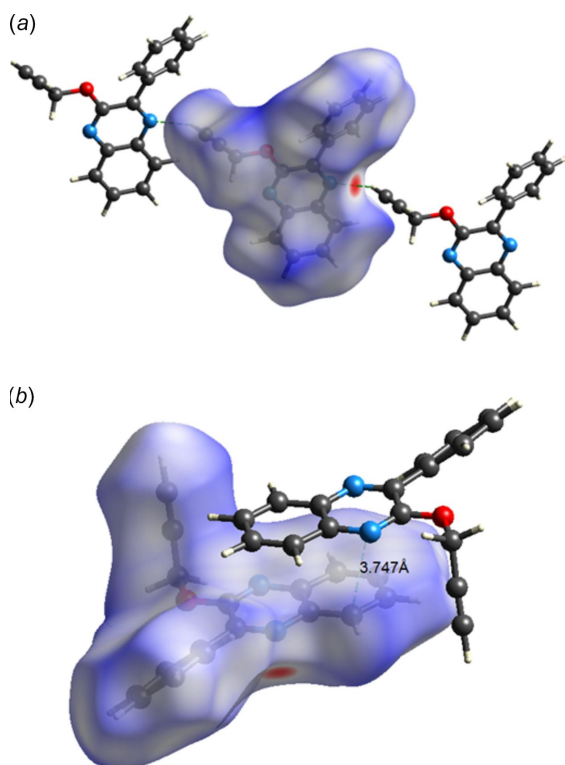


Figure 4
The Hirshfeld surface plotted over d_{norm} in the range -0.2356 to 1.4819 in arbitrary units with (a) two neighboring hydrogen bonded molecules and (b) one neighboring π -stacked molecule.

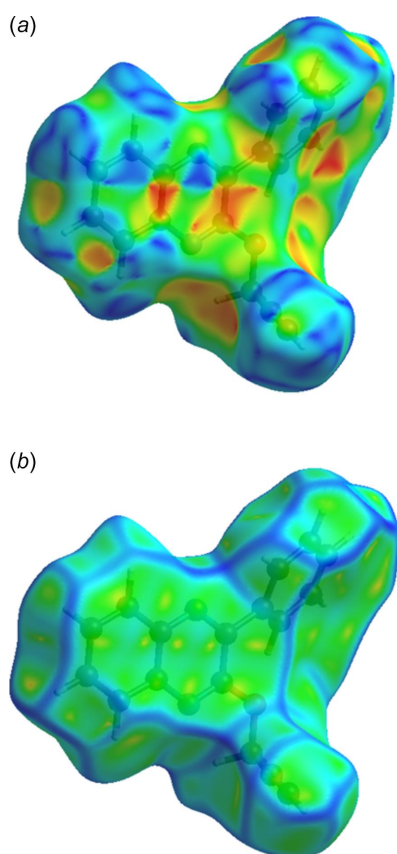


Figure 5
The Hirshfeld surface plotted over (a) shape-index and (b) curvature.

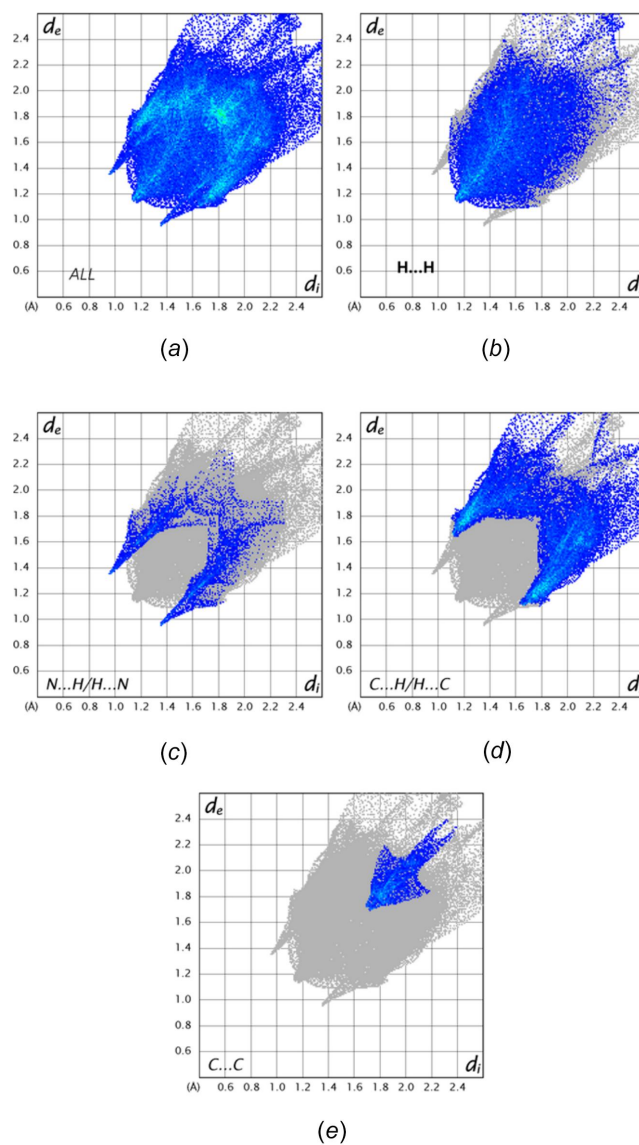


Figure 6
2D fingerprint plots for (a) all intermolecular interactions, and delineated into (b) $\text{H}\cdots\text{H}$, (c) $\text{N}\cdots\text{H}/\text{H}\cdots\text{N}$, (d) $\text{C}\cdots\text{H}/\text{H}\cdots\text{C}$ and (e) $\text{C}\cdots\text{C}$ interactions.

such contacts with distances slightly shorter than to slightly longer than the sum of the respective van der Waals radii.

4. Database survey

A search of the Cambridge Structural Database (CSD, updated to January 2024; Groom *et al.*, 2016) using fragment **A** (Fig. 7, R = any atom), yielded seven hits similar to the title molecule, *viz.* FACPEI with R = benzyl (Abad *et al.*, 2020), 3-(2-oxo-3-phenylquinoxalin-1(2*H*)-yl)propyl (KOPKAF; Abad *et al.*, 2024) and 2-(2-oxooxazolidin-3-yl)ethyl [monoclinic form (UREREP01; Daouda *et al.*, 2020) and orthorhombic form (UREREP; Daouda *et al.*, 2011)]. The last three are **B** (BZOQUX10; Oberti *et al.*, 1978), **C** (YEFDUK; Moreau *et al.*, 2012) and **D** (VAQNAE; Kumar *et al.*, 2012). The quinoxaline moiety is closest to planar in BZOQUX10

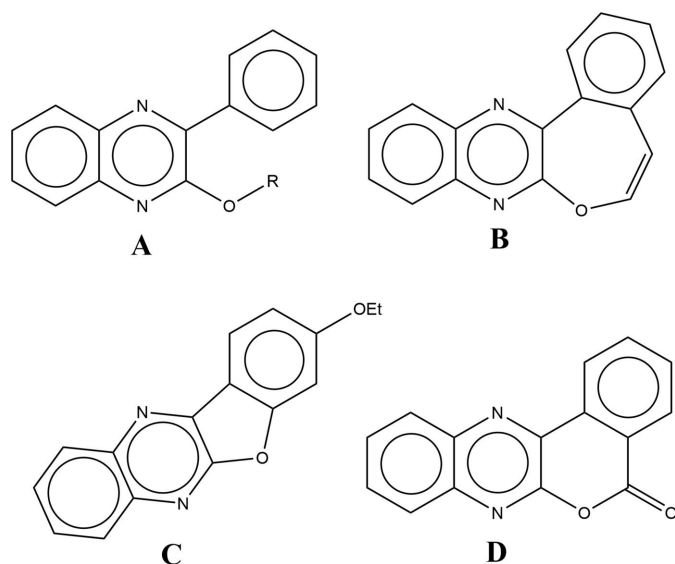


Figure 7
Search fragment (A), BZOQUX10 (B), VAQNAE (C) and YEFDUK (D).

[dihedral angle between constituent planes = $1.13 (1)^\circ$], while in UREREP it is furthest from planar [dihedral angle between constituent planes = $3.34 (16)^\circ$]. These two compounds also exhibit the smallest [$30.60 (1)^\circ$] and largest [$38.72 (16)^\circ$] angles of inclination of the phenyl group. The other structures show intermediate values for both angles, except for YEFDUK and VAQNAE where this angle is less than 5° because the phenyl ring is part of a six- or five-membered ring fused to the nitrogen-containing heterocycle.

5. Synthesis and crystallization

3-Phenylquinoxalin-2(1*H*)-one (1 g, 4.5 mmol), 3-bromoprop-1-yne (0.96 mL, 9 mmol), and potassium carbonate (0.931 g, 6.75 mmol) with an amount of catalytic tetra-*n*-butylammonium bromide (0.29 g, 0.9 mmol) were stirred in *N,N*-dimethylformamide (DMF) (20 mL) for 48 h (Fig. 1). The solution was filtered, and the solvent was removed under vacuum. Dichloromethane (20 mL) was added, and the solution was filtered. The residue was chromatographed on a silica gel column (hexane/ethyl acetate: 9.5/0.5, as mobile phase) to give two fractions. The first fraction was purified by recrystallization in ethanol to afford colorless crystals with a yield of 28.3% (*O*-alkylated isomer, title compound) while recrystallization of the second fraction gave a yellowish powder with a yield of 53.5% (*N*-alkylated isomer).

***O*-alkylated isomer:** Yield: 28.3%, m.p. = 370–372 K, ^1H NMR (300 MHz, CDCl_3) δ ppm: 2.55 (*t*, 1H, *CH*, $J = 3\text{Hz}$); 5.265 (*d*, 2H, $\text{O}-\text{CH}_2$, $J = 3\text{Hz}$); 7.55–8.20 (*m*, 9H, CH_{arom}); ^{13}C NMR (75 MHz, CDCl_3) δ ppm: 53.93 ($\text{O}-\text{CH}_2$); 74.85 (*CH*); 78.57 (*-C*); 126.85, 127.22, 128.31, 129.06, 129.75, 129.82, 129.86 (CH_{arom}); 136.77, 139.35, 139.49, 146.29 (*Cq*); 154.11 (*Cq}-\text{O}*).

***N*-alkylated isomer:** Yield 53.5%, m.p. = 385–387 K, ^1H NMR (300 MHz, CDCl_3) δ ppm: 2.35 (*t*, H, *CH*, $J = 3\text{Hz}$); 5.155

Table 2
Experimental details.

Crystal data	
Chemical formula	$\text{C}_{17}\text{H}_{12}\text{N}_2\text{O}$
M_r	260.29
Crystal system, space group	Triclinic, $P\bar{1}$
Temperature (K)	120
a, b, c (\AA)	8.4614 (14), 9.0947 (15), 9.5360 (16)
α, β, γ ($^\circ$)	87.739 (2), 72.963 (2), 69.028 (2)
V (\AA^3)	653.39 (19)
Z	2
Radiation type	Mo $K\alpha$
μ (mm^{-1})	0.08
Crystal size (mm)	$0.34 \times 0.33 \times 0.14$
Data collection	
Diffractometer	Bruker SMART APEX CCD
Absorption correction	Multi-scan (<i>SADABS</i> ; Krause <i>et al.</i> , 2015)
$T_{\text{min}}, T_{\text{max}}$	0.91, 0.99
No. of measured, independent and observed [$I > 2\sigma(I)$] reflections	12629, 3456, 2869
R_{int}	0.026
$(\sin \theta/\lambda)_{\text{max}}$ (\AA^{-1})	0.684
Refinement	
$R[F^2 > 2\sigma(F^2)], wR(F^2), S$	0.044, 0.139, 1.17
No. of reflections	3456
No. of parameters	181
H-atom treatment	H-atom parameters constrained
$\Delta\rho_{\text{max}}, \Delta\rho_{\text{min}}$ (e \AA^{-3})	0.42, -0.24

Computer programs: *APEX3* and *SAINT* (Bruker, 2016), *SHELXT* (Sheldrick, 2015a), *SHELXL2019/1* (Sheldrick, 2015a), *DIAMOND* (Brandenburg & Putz, 2012) and *SHELXTL* (Sheldrick, 2008).

(*d*, 2H, $\text{N}-\text{CH}_2$, $J = 3\text{Hz}$); 7.41–8.36 (*m*, 9H, CH_{arom}); ^{13}C NMR (75 MHz, CDCl_3) δ ppm: 31.69 ($\text{N}-\text{CH}_2$); 73.19 (*CH*); 76.96 (*-C*); 114.07, 124.15, 128.13, 129.61, 130.45, 130.53, 130.63 (CH_{arom}); 131.87, 133.31, 135.78, 153.72 (*Cq*); 153.98 ($\text{C}=\text{O}$).

6. Refinement

Crystal data, data collection and structure refinement details are summarized in Table 2. Hydrogen atoms were included as riding contributions in idealized positions with isotropic displacement parameters tied to those of the attached atoms.

Acknowledgements

JTM thanks Tulane University for support of the Tulane Crystallography Laboratory.

References

- Abad, N., Lgaz, H., Atioglu, Z., Akkurt, M., Mague, J. T., Ali, I. H., Chung, I.-M., Salghi, R., Essassi, E. M. & Ramli, Y. (2020). *J. Mol. Struct.* **1221**, 128727.
- Abad, N., Mague, J. T., Alsubari, A., Essassi, E. M., Alzahrani, A. Y. A. & Ramli, Y. (2024). *Acta Cryst.* **E80**, 300–304.
- Brandenburg, K. & Putz, H. (2012). *DIAMOND*. Crystal Impact GbR, Bonn, Germany.
- Bruker (2016). *APEX3* and *SAINT*, Bruker AXS, Madison, Wisconsin, USA.

- Daouda, B., Brelot, L., Doumbia, M. L., Essassi, E. M. & Ng, S. W. (2011). *Acta Cryst.* **E67**, o1235.
- Daouda, B., Doumbia, M. L., Hökelek, T., Zemmouri, F., Claude, K. A. L., Douira, A., Sebbar, N. K. & Essassi, E. M. (2020). *J. Mar. Chim. Heterocycl.* **19**, 55–69.
- Groom, C. R., Bruno, I. J., Lightfoot, M. P. & Ward, S. C. (2016). *Acta Cryst.* **B72**, 171–179.
- Krause, L., Herbst-Irmer, R., Sheldrick, G. M. & Stalke, D. (2015). *J. Appl. Cryst.* **48**, 3–10.
- Kumar, K. S., Adepur, R., Kapavarapu, R., Rambabu, D., Krishna, G. R., Reddy, C. M., Priya, K. K. K., Parsa, V. L. & Pal, M. (2012). *Tetrahedron Lett.* **53**, 1134–1138.
- Lgaz, H., ELaoufir, Y., Ramli, Y., Larouj, M., Zarrok, H., Salghi, R., Zarrouk, A., Elmidaoui, A., Guenbour, A., Essassi, E. M. & Oudda, H. (2015). *Der. Pharma Chem.* **7**, 36–45.
- Missioui, M., Said, M., Demirtaş, G., Mague, J. T., Al-Sulami, A., Al-Kaff, N. S. & Ramli, Y. (2022). *Arab. J. Chem.* **15**, 103595.
- Moreau, S., Desplat, V., Savrimoutou, S., Massip, S., Deleris, G. & Guillon, J. (2012). *Compte Rend. Chim.* **15**, 753–757.
- Oberti, R., Coda, A., Incoccia, L. & Comin, F. (1978). *Acta Cryst.* **B34**, 1544–1548.
- Ramli, Y. & Essassi, E. M. (2015). *Adv. Chem. Res.* **27**, 109–160.
- Sheldrick, G. M. (2008). *Acta Cryst.* **A64**, 112–122.
- Sheldrick, G. M. (2015a). *Acta Cryst.* **A71**, 3–8.
- Sheldrick, G. M. (2015b). *Acta Cryst.* **C71**, 3–8.
- Spackman, P. R., Turner, M. J., McKinnon, J. J., Wolff, S. K., Grimwood, D. J., Jayatilaka, D. & Spackman, M. A. (2021). *J. Appl. Cryst.* **54**, 1006–1011.
- Spek, A. L. (2020). *Acta Cryst.* **E76**, 1–11.
- Tan, S. L., Jotani, M. M. & Tiekink, E. R. T. (2019). *Acta Cryst.* **E75**, 308–318.

supporting information

Acta Cryst. (2024). E80, 383-387 [https://doi.org/10.1107/S2056989024002585]

Synthesis, crystal structure and Hirshfeld surface analysis of 2-phenyl-3-(prop-2-yn-1-yloxy)quinoxaline

Nadeem Abad, Joel T. Mague, Abdulsalam Alsubari, El Mokhtar Essassi, Mehrdad Pourayoubi, Abdullah Yahya Abdullah Alzahrani and Youssef Ramli

Computing details

2-Phenyl-3-(prop-2-yn-1-yloxy)quinoxaline

Crystal data

$C_{17}H_{12}N_2O$

$M_r = 260.29$

Triclinic, $P\bar{1}$

$a = 8.4614$ (14) Å

$b = 9.0947$ (15) Å

$c = 9.5360$ (16) Å

$\alpha = 87.739$ (2)°

$\beta = 72.963$ (2)°

$\gamma = 69.028$ (2)°

$V = 653.39$ (19) Å³

$Z = 2$

$F(000) = 272$

$D_x = 1.323$ Mg m⁻³

Mo $K\alpha$ radiation, $\lambda = 0.71073$ Å

Cell parameters from 6800 reflections

$\theta = 2.2$ – 29.1 °

$\mu = 0.08$ mm⁻¹

$T = 120$ K

Thick plate, colourless

$0.34 \times 0.33 \times 0.14$ mm

Data collection

Bruker SMART APEX CCD

diffractometer

Radiation source: fine-focus sealed tube

Graphite monochromator

Detector resolution: 8.3333 pixels mm⁻¹

φ and ω scans

Absorption correction: multi-scan

(*SADABS*; Krause *et al.*, 2015)

$T_{\min} = 0.91$, $T_{\max} = 0.99$

12629 measured reflections

3456 independent reflections

2869 reflections with $I > 2\sigma(I)$

$R_{\text{int}} = 0.026$

$\theta_{\max} = 29.1$ °, $\theta_{\min} = 2.2$ °

$h = -11 \rightarrow 11$

$k = -12 \rightarrow 12$

$l = -13 \rightarrow 12$

Refinement

Refinement on F^2

Least-squares matrix: full

$R[F^2 > 2\sigma(F^2)] = 0.044$

$wR(F^2) = 0.139$

$S = 1.17$

3456 reflections

181 parameters

0 restraints

Primary atom site location: dual

Secondary atom site location: difference Fourier map

Hydrogen site location: inferred from neighbouring sites

H-atom parameters constrained

$w = 1/[\sigma^2(F_o^2) + (0.0919P)^2]$

where $P = (F_o^2 + 2F_c^2)/3$

$(\Delta/\sigma)_{\max} < 0.001$

$\Delta\rho_{\max} = 0.42$ e Å⁻³

$\Delta\rho_{\min} = -0.24$ e Å⁻³

Special details

Experimental. The diffraction data were obtained from 3 sets of 400 frames, each of width 0.5° in ω , collected at $\varphi = 0.00, 90.00$ and 180.00° and 2 sets of 800 frames, each of width 0.45° in φ , collected at $\omega = -30.00$ and 210.00° . The scan time was 10 sec/frame.

Geometry. All esds (except the esd in the dihedral angle between two l.s. planes) are estimated using the full covariance matrix. The cell esds are taken into account individually in the estimation of esds in distances, angles and torsion angles; correlations between esds in cell parameters are only used when they are defined by crystal symmetry. An approximate (isotropic) treatment of cell esds is used for estimating esds involving l.s. planes.

Refinement. Refinement of F^2 against ALL reflections. The weighted R-factor wR and goodness of fit S are based on F^2 , conventional R-factors R are based on F, with F set to zero for negative F^2 . The threshold expression of $F^2 > 2\sigma(F^2)$ is used only for calculating R-factors(gt) etc. and is not relevant to the choice of reflections for refinement. R-factors based on F^2 are statistically about twice as large as those based on F, and R-factors based on ALL data will be even larger. H-atoms attached to carbon were placed in calculated positions (C—H = 0.95 - 1.00 Å). All were included as riding contributions with isotropic displacement parameters 1.2 - 1.5 times those of the attached atoms.

Fractional atomic coordinates and isotropic or equivalent isotropic displacement parameters (\AA^2)

	x	y	z	$U_{\text{iso}}^*/U_{\text{eq}}$
O1	0.70891 (9)	0.56445 (8)	0.38257 (7)	0.02033 (18)
N1	0.46180 (11)	0.60416 (9)	0.30849 (8)	0.01784 (19)
N2	0.63397 (10)	0.29963 (9)	0.16411 (8)	0.01617 (19)
C1	0.46804 (12)	0.39265 (11)	0.15776 (10)	0.0163 (2)
C2	0.38348 (13)	0.33437 (11)	0.07839 (10)	0.0202 (2)
H2	0.443192	0.233469	0.026117	0.024*
C3	0.21438 (13)	0.42397 (12)	0.07686 (11)	0.0221 (2)
H3	0.157226	0.384741	0.023461	0.027*
C4	0.12524 (13)	0.57396 (12)	0.15423 (11)	0.0227 (2)
H4	0.007481	0.633952	0.154015	0.027*
C5	0.20634 (13)	0.63425 (11)	0.22970 (10)	0.0206 (2)
H5	0.145802	0.736230	0.279815	0.025*
C6	0.37993 (12)	0.54442 (11)	0.23271 (10)	0.0168 (2)
C7	0.61911 (12)	0.51363 (11)	0.31114 (9)	0.0161 (2)
C8	0.71038 (12)	0.35506 (10)	0.23996 (9)	0.0153 (2)
C9	0.62072 (14)	0.72174 (11)	0.45585 (10)	0.0220 (2)
H9A	0.664895	0.726667	0.540217	0.026*
H9B	0.491675	0.744261	0.494533	0.026*
C10	0.65155 (13)	0.84189 (11)	0.35597 (10)	0.0203 (2)
C11	0.67695 (14)	0.94264 (12)	0.27984 (11)	0.0260 (2)
H11	0.697268	1.023246	0.218929	0.031*
C12	0.88656 (12)	0.24852 (11)	0.24864 (10)	0.0164 (2)
C13	0.93639 (13)	0.24226 (12)	0.37693 (10)	0.0217 (2)
H13	0.860641	0.313948	0.459583	0.026*
C14	1.09717 (14)	0.13079 (12)	0.38327 (11)	0.0251 (2)
H14	1.129576	0.125487	0.471192	0.030*
C15	1.21016 (13)	0.02769 (12)	0.26279 (12)	0.0259 (2)
H15	1.320346	-0.047128	0.267536	0.031*
C16	1.16184 (13)	0.03400 (12)	0.13478 (11)	0.0243 (2)
H16	1.239339	-0.036390	0.051699	0.029*
C17	1.00061 (13)	0.14291 (11)	0.12807 (10)	0.0198 (2)

H17 0.967552 0.145639 0.040722 0.024*

Atomic displacement parameters (Å²)

	U^{11}	U^{22}	U^{33}	U^{12}	U^{13}	U^{23}
O1	0.0248 (4)	0.0157 (3)	0.0240 (4)	-0.0084 (3)	-0.0109 (3)	0.0001 (3)
N1	0.0202 (4)	0.0157 (4)	0.0170 (4)	-0.0062 (3)	-0.0051 (3)	0.0012 (3)
N2	0.0171 (4)	0.0152 (4)	0.0165 (4)	-0.0063 (3)	-0.0050 (3)	0.0025 (3)
C1	0.0164 (4)	0.0157 (4)	0.0162 (4)	-0.0062 (3)	-0.0042 (3)	0.0038 (3)
C2	0.0216 (5)	0.0182 (5)	0.0222 (5)	-0.0084 (4)	-0.0072 (4)	0.0013 (4)
C3	0.0223 (5)	0.0253 (5)	0.0238 (5)	-0.0121 (4)	-0.0102 (4)	0.0049 (4)
C4	0.0170 (5)	0.0259 (5)	0.0234 (5)	-0.0058 (4)	-0.0069 (4)	0.0067 (4)
C5	0.0198 (5)	0.0182 (5)	0.0198 (4)	-0.0031 (4)	-0.0049 (4)	0.0025 (4)
C6	0.0181 (4)	0.0165 (4)	0.0151 (4)	-0.0062 (4)	-0.0041 (3)	0.0024 (3)
C7	0.0193 (5)	0.0155 (4)	0.0143 (4)	-0.0079 (4)	-0.0044 (3)	0.0024 (3)
C8	0.0171 (4)	0.0146 (4)	0.0144 (4)	-0.0066 (3)	-0.0041 (3)	0.0026 (3)
C9	0.0307 (5)	0.0184 (5)	0.0189 (4)	-0.0114 (4)	-0.0068 (4)	-0.0011 (4)
C10	0.0202 (5)	0.0182 (5)	0.0218 (4)	-0.0055 (4)	-0.0064 (4)	-0.0028 (4)
C11	0.0289 (6)	0.0208 (5)	0.0276 (5)	-0.0092 (4)	-0.0074 (4)	0.0020 (4)
C12	0.0170 (4)	0.0140 (4)	0.0203 (4)	-0.0072 (3)	-0.0066 (4)	0.0033 (3)
C13	0.0230 (5)	0.0217 (5)	0.0202 (4)	-0.0065 (4)	-0.0081 (4)	0.0016 (4)
C14	0.0277 (5)	0.0247 (5)	0.0286 (5)	-0.0095 (4)	-0.0171 (4)	0.0056 (4)
C15	0.0204 (5)	0.0205 (5)	0.0385 (6)	-0.0054 (4)	-0.0142 (4)	0.0049 (4)
C16	0.0203 (5)	0.0188 (5)	0.0292 (5)	-0.0025 (4)	-0.0064 (4)	-0.0018 (4)
C17	0.0210 (5)	0.0174 (4)	0.0218 (4)	-0.0065 (4)	-0.0081 (4)	0.0012 (4)

Geometric parameters (Å, °)

O1—C7	1.3544 (11)	C8—C12	1.4832 (12)
O1—C9	1.4493 (12)	C9—C10	1.4648 (13)
N1—C7	1.2976 (12)	C9—H9A	0.9900
N1—C6	1.3751 (12)	C9—H9B	0.9900
N2—C8	1.3158 (11)	C10—C11	1.1874 (14)
N2—C1	1.3733 (11)	C11—H11	0.9500
C1—C2	1.4094 (12)	C12—C17	1.3961 (13)
C1—C6	1.4145 (13)	C12—C13	1.3991 (12)
C2—C3	1.3741 (13)	C13—C14	1.3922 (14)
C2—H2	0.9500	C13—H13	0.9500
C3—C4	1.4110 (15)	C14—C15	1.3831 (16)
C3—H3	0.9500	C14—H14	0.9500
C4—C5	1.3709 (14)	C15—C16	1.3895 (14)
C4—H4	0.9500	C15—H15	0.9500
C5—C6	1.4105 (13)	C16—C17	1.3876 (13)
C5—H5	0.9500	C16—H16	0.9500
C7—C8	1.4525 (13)	C17—H17	0.9500
C7—O1—C9	117.08 (7)	O1—C9—C10	111.63 (8)
C7—N1—C6	117.06 (8)	O1—C9—H9A	109.3

C8—N2—C1	118.73 (8)	C10—C9—H9A	109.3
N2—C1—C2	119.45 (8)	O1—C9—H9B	109.3
N2—C1—C6	120.70 (8)	C10—C9—H9B	109.3
C2—C1—C6	119.83 (8)	H9A—C9—H9B	108.0
C3—C2—C1	119.79 (9)	C11—C10—C9	177.21 (10)
C3—C2—H2	120.1	C10—C11—H11	180.0
C1—C2—H2	120.1	C17—C12—C13	119.09 (8)
C2—C3—C4	120.30 (9)	C17—C12—C8	118.53 (8)
C2—C3—H3	119.8	C13—C12—C8	122.21 (8)
C4—C3—H3	119.8	C14—C13—C12	119.89 (9)
C5—C4—C3	120.87 (9)	C14—C13—H13	120.1
C5—C4—H4	119.6	C12—C13—H13	120.1
C3—C4—H4	119.6	C15—C14—C13	120.63 (9)
C4—C5—C6	119.81 (9)	C15—C14—H14	119.7
C4—C5—H5	120.1	C13—C14—H14	119.7
C6—C5—H5	120.1	C14—C15—C16	119.73 (9)
N1—C6—C5	120.06 (9)	C14—C15—H15	120.1
N1—C6—C1	120.56 (8)	C16—C15—H15	120.1
C5—C6—C1	119.38 (9)	C17—C16—C15	120.12 (9)
N1—C7—O1	120.57 (8)	C17—C16—H16	119.9
N1—C7—C8	123.68 (8)	C15—C16—H16	119.9
O1—C7—C8	115.75 (8)	C16—C17—C12	120.54 (8)
N2—C8—C7	119.21 (8)	C16—C17—H17	119.7
N2—C8—C12	116.98 (8)	C12—C17—H17	119.7
C7—C8—C12	123.80 (8)		
<hr/>			
C8—N2—C1—C2	-179.28 (8)	C1—N2—C8—C7	-1.53 (13)
C8—N2—C1—C6	-0.75 (13)	C1—N2—C8—C12	177.76 (7)
N2—C1—C2—C3	177.16 (8)	N1—C7—C8—N2	2.22 (14)
C6—C1—C2—C3	-1.38 (14)	O1—C7—C8—N2	-177.66 (7)
C1—C2—C3—C4	0.06 (14)	N1—C7—C8—C12	-177.02 (8)
C2—C3—C4—C5	1.26 (15)	O1—C7—C8—C12	3.10 (13)
C3—C4—C5—C6	-1.21 (15)	C7—O1—C9—C10	-87.00 (10)
C7—N1—C6—C5	177.76 (7)	N2—C8—C12—C17	33.33 (12)
C7—N1—C6—C1	-1.98 (14)	C7—C8—C12—C17	-147.42 (9)
C4—C5—C6—N1	-179.86 (8)	N2—C8—C12—C13	-141.76 (9)
C4—C5—C6—C1	-0.13 (14)	C7—C8—C12—C13	37.49 (13)
N2—C1—C6—N1	2.63 (14)	C17—C12—C13—C14	-0.54 (14)
C2—C1—C6—N1	-178.84 (8)	C8—C12—C13—C14	174.53 (8)
N2—C1—C6—C5	-177.10 (8)	C12—C13—C14—C15	1.21 (15)
C2—C1—C6—C5	1.42 (14)	C13—C14—C15—C16	-0.83 (16)
C6—N1—C7—O1	179.51 (7)	C14—C15—C16—C17	-0.23 (15)
C6—N1—C7—C8	-0.37 (14)	C15—C16—C17—C12	0.90 (14)
C9—O1—C7—N1	0.65 (13)	C13—C12—C17—C16	-0.51 (14)
C9—O1—C7—C8	-179.47 (7)	C8—C12—C17—C16	-175.76 (8)

Hydrogen-bond geometry (Å, °)

<i>D</i> —H··· <i>A</i>	<i>D</i> —H	H··· <i>A</i>	<i>D</i> ··· <i>A</i>	<i>D</i> —H··· <i>A</i>
C11—H11···N2 ⁱ	0.95	2.44	3.3164 (14)	153

Symmetry code: (i) *x*, *y*+1, *z*.